ISBN: 978-3-95450-202-8 doi:10.18429/JACoW-HB2018-MOP2WA03

EXPERIMENTS AND THEORY ON BEAM STABILIZATION WITH SECOND-ORDER CHROMATICITY

M. Schenk*[1], X. Buffat, L. R. Carver, K. Li, E. Métral
European Organization for Nuclear Research (CERN), CH-1211 Geneva, Switzerland
[1]also at École Polytechnique Fédérale de Lausanne (EPFL), CH-1015 Lausanne, Switzerland
A. Maillard, École Normale Supérieure (ENS), F-75230 Paris, France

Abstract

This study reports on an alternative method to generate transverse Landau damping to suppress coherent instabilities in circular accelerators. The incoherent betatron tune spread can be produced through detuning with longitudinal rather than transverse action. This approach is motivated by the high-brightness, low transverse emittance beams in future colliders where detuning with transverse amplitude will be less effective. Detuning with longitudinal action can be introduced with a radio frequency (rf) quadrupole, or similarly, using second-order chromaticity. The latter was enhanced in the Large Hadron Collider (LHC) at CERN and experimental results on single-bunch stabilization are briefly recapped. The observations are interpreted analytically by extending the Vlasov formalism to include nonlinear chromaticity. Finally, the newly developed theory is benchmarked against circulant matrix and particle tracking models.

INTRODUCTION

Due to the strongly reduced transverse emittances of the beams in the Future Circular hadron Collider (FCC-hh), generating a betatron tune spread with magnetic octupoles for Landau damping of transverse dipole modes is ineffective, in particular at high energy [1, 2]. Betatron detuning with longitudinal amplitude introduced by means of an rf quadrupole is hence under study as a potential alternative [3]. Numerical studies performed with the *PyHEADTAIL* tracking code demonstrate that such an rf device can indeed provide beam stabilization [4, 5].

It was shown in Ref. [6] that second-order chromaticity (Q'') mimics the effect of an rf quadrupole at first order. Measurements were performed in the LHC where Q'' was enhanced and single bunches were stabilized at 6.5 TeV through detuning with longitudinal amplitude [7, 8]. *PyHEADTAIL* showed a very good agreement with the data, confirming the correct modelling of Landau damping from an rf quadrupole or nonlinear chromaticity in the code [6]. Both simulations and experiments indicate that Q'' introduces two beam dynamics effects: (i) it changes the effective impedance and hence the transverse dipole modes and their associated coherent frequencies, and (ii) it generates a betatron tune spread depending on the longitudinal amplitude and therefore Landau damping.

The objective of this study is to present the progress made on the development of the Vlasov theory for nonlinear chromaticity and to confirm analytically the two effects that were observed in the LHC. First, the main results and conclusions from the experiments are recapped before briefly explaining how the Vlasov formalism was extended to include nonlinear chromaticity. Finally, results from numerical studies with *PyHEADTAIL* and the circulant matrix solver *BimBim* are discussed to demonstrate the validity of the developed theory [9, 10]. Only the main results for airbag and Gaussian beams are presented here, with specific approximations on the impedance model. A complete study including detailed derivations and providing considerably more information on the benchmarks is currently in preparation and will be submitted to a peer-reviewed journal in the near future.

LHC EXPERIMENTS

LHC Single-Bunch Stability

At 6.5 TeV, with design bunch parameters, first-order chromaticity $Q'_{x,y}$ between 11 and 14 units, and the transverse feedback system active with a damping time of approximately 100 turns, the main transverse single-bunch instability in the LHC is a horizontal head-tail mode with azimuthal and radial numbers $l = 0$ and $m = 2$ respectively [11, 12]. During routine operation this instability is mitigated by means of the Landau octupoles [13]. The minimum current required for stabilization was measured to be $I_{\mathrm{oct}}^{\mathrm{meas}} = 96^{+29}_{-10}$ A. Using a detailed LHC impedance model [14], *PyHEADTAIL* predicts the correct instability threshold ($I_{\mathrm{oct}}^{\mathrm{sim}} = 107.5 \pm 2.5$ A) and the right azimuthal and radial numbers of the head-tail mode, confirming the high reliability of the numerical model.

Second-Order Chromaticity Study

The LHC main sextupoles are grouped into focusing and defocusing families and each of them is split further into two subfamilies interleaved by a phase advance of about π. The four groups can be powered individually for each of the eight machine sectors which makes it possible to control the second-order chromaticity independently in the two transverse planes and without affecting $Q'_{x,y}$. For each of the two beams, two orthogonal (nonlinear) knobs QPPX and QPPY were defined to enhance respectively Q''_x and Q''_y.

The experiment was performed with two bunches in each of the two beams at 6.5 TeV. The Landau octupoles were initially powered with $I_{\mathrm{oct}} = 320$ A to ensure beam stability. The settings for QPPX and QPPY were determined using MAD-X to introduce $Q''_{x,y} \approx -4 \times 10^4$ in both beams once

* michael.schenk@cern.ch

ISBN: 978-3-95450-202-8 doi:10.18429/JACoW-HB2018-MOP2WA03

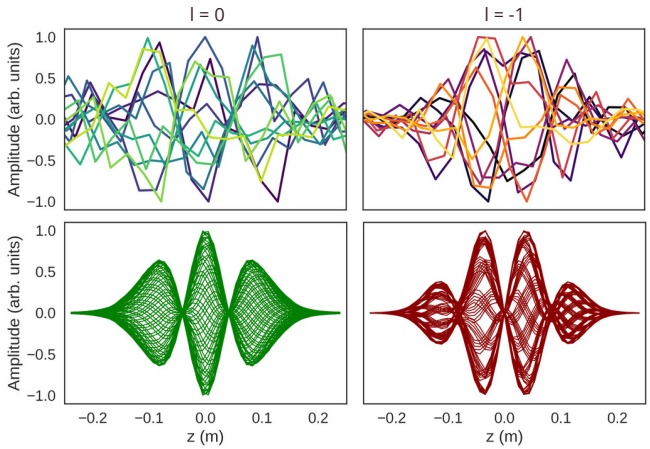

Figure 1: Comparison of the two horizontal head-tail modes observed in the LHC (top) and in *PyHEADTAIL* simulations (bottom) without (left) and with (right) Q''_x.

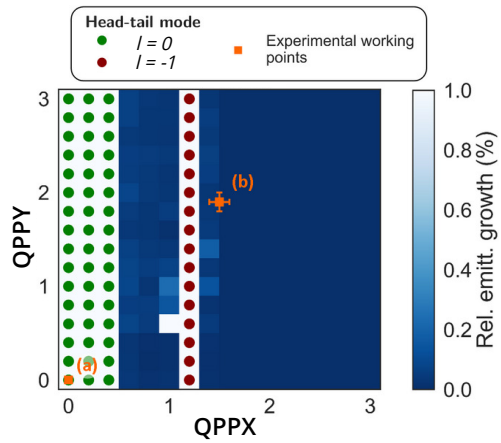

Figure 2: *PyHEADTAIL* study showing the predicted horizontal head-tail instabilities and the emittance growth in the QPPX vs. QPPY plane. Labels (a) and (b) denote the two experimental working points.

the current in the Landau octupoles would be reduced to zero [15]. The reason for using negative Q'' is that it provides a higher stabilizing efficiency for the head-tail mode observed in the LHC which is characterized by a negative real coherent tune shift [6, 16]. This is due to the strong asymmetry of the tune spreads and hence of the stability boundary diagrams introduced by Q'' (see theory below). As soon as the targeted sextupole settings were reached, the current in the Landau octupoles was decreased in steps of 40 A. At $I_{\mathrm{oct}} = 40$ A all four bunches were still stable. At this stage $Q''_{x,y}$ measurements were performed that showed a good agreement with MAD-X predictions hence demonstrating that Q'' is well-controlled in the machine [6]. Once the Landau octupole current was reduced to 0 A, a horizontal instability occurred in one of the four bunches while the other three remained stable. The reason why only one bunch went unstable was its significantly higher intensity compared to the second bunch in the same beam [8]. The observed instability was now no longer a head-tail mode $(l,m) = (0,2)$, but instead had mode numbers $(l,m) = (-1,3)$. Figure 1 (top) displays the measured head-tail patterns without (left) and with (right) Q'', acquired by the Head-Tail Monitor [17]. The fact that the bunches were stable at significantly reduced, or even zero octupole current indicated a strong Landau damping effect from Q'', later confirmed by tracking simulations.

PyHEADTAIL was used to interpret the experimental observations made. 4×10^5 macroparticles were tracked over 1.8×10^6 turns, again using the detailed LHC impedance model. Figure 2 summarizes the main results. The color code shows the relative emittance growth over the simulation period in %, where 'blue' is stable and 'white' unstable. The dots represent the azimuthal mode number of the instability predicted for each setting of the Q'' knobs. Labels (a) and (b) correspond to the two experimental working points, respectively with and without Q''. The plot shows that large regions of stability are created in the QPPX vs. QPPY plane thanks to Landau damping from Q''. The two main stable areas are, however, separated by an unstable band indicating a head-tail mode $l = -1$ (red dots). This is a consequence of Q'' changing the effective impedance and hence the head-tail modes as discussed analytically in the following section. The first unstable band observed at low values of Q'' is the mode $l = 0$ (green dots), consistent with experimental observations made in absence of Q''. The stable region between the two unstable bands arises from sufficient Landau damping of both modes. The further increase of Q'', however, leads to a change of the effective impedance, causing a loss of Landau damping for the $l = -1$ mode. For even larger amounts of Q'', all the instabilities are suppressed. Additionally, working point (b) lies close to the second unstable band. This is consistent with experimental data which clearly show that the observed horizontal instability is indeed of mode -1. Overall, the experimental results, and in particular the Head-Tail Monitor signals, are in excellent agreement with the simulations, displayed in Fig. 1 (bottom).

In the following section, the existing Vlasov theory will be extended to include the effects of nonlinear chromaticity, making it possible to confirm the interpretation of the experimental observations analytically.

VLASOV THEORY

Vlasov's equation in transverse (q,θ) and longitudinal (r,ϕ) polar coordinates reads [18]

$$\left[\partial_s + \frac{1}{c}\,\omega_\beta(\delta)\,\partial_\theta + \frac{\omega_s}{c}\partial_\phi + \frac{F_y}{E}\partial_{p_y}\right]\Psi = 0, \qquad (1)$$

where Ψ is the particle distribution in 4D phase space (including the longitudinal and *one* transverse plane), s the longitudinal position of the bunch along the accelerator, c the speed of light, E the total energy of the beam particles, F_y the transverse force representing here the effect of transverse dipolar wakefields, $p_y(q,\theta)$ the transverse momentum, δ the relative longitudinal momentum error, and ω_s the synchrotron frequency. Nonlinear chromaticity terms up to

ISBN: 978-3-95450-202-8 doi:10.18429/JACoW-HB2018-MOP2WA03

order m are included in the equation through a dependency of the betatron frequency on δ

$$\omega_\beta(\delta) = \omega_{\beta,0} + \Delta\omega_\beta(\delta) = \omega_{\beta,0} \sum_{k=0}^{m} \frac{\xi^{(k)}}{k!}\delta^k, \qquad (2)$$

with $\omega_{\beta,0}$ the unperturbed betatron frequency, and

$$\xi^{(n)} = \frac{1}{\omega_{\beta,0}} \frac{\partial^n \omega_\beta}{\partial \delta^n}\bigg|_{\delta=0} \qquad (3)$$

the nonlinear chromaticity of order n.

To simplify the Vlasov equation and to find the solutions Ψ of the collective transverse dipole modes, one proceeds in a similar way as explained in Ref. [18], Eqs. (6.166) to (6.179), while allowing for an arbitrary dependence of the betatron frequency on the longitudinal momentum deviation. First, Ψ is described as a sum of a stationary solution and a perturbation term $\Psi = \Psi_0 + \Psi_1$, where $\Psi_0 = g_0(r) f_0(q)$ and $\Psi_1 = -D g_1(r,\phi)\, f_0'(q)\, e^{i\theta}\, e^{-i\Omega s/c}$. g_0 and g_1 are the stationary and perturbed longitudinal distributions respectively, and f_0 is the transverse stationary distribution. D is the dipolar moment of the perturbed distribution and Ω the complex coherent frequency associated with the mode. Using this approach, the Vlasov equation can be reduced such that it involves only longitudinal coordinates. The wakefield term is expressed in frequency domain using the transverse dipolar impedance $Z_1^\perp(\omega)$ and one can obtain an equation similar to (6.174) in Ref. [18]. From this point onwards, one deviates from the path described in Ref. [18] and instead rewrites the Vlasov equation in terms of the functions

$$G_1(r,\phi) \doteq g_1(r,\phi)\, e^{\frac{i}{\omega_s}\int_0^\phi \Delta\omega_\beta(\delta(r,u))\,du}. \qquad (4)$$

They can be further decomposed into the azimuthal eigenmodes $G_1^l(r,\phi)$ (with eigenvalues $\Omega^{(l)}$) of the *free* ($Z_1^\perp \equiv 0$) Vlasov equation

$$\begin{aligned} G_1^l(r,\phi) &= R_l(r)\, e^{i\left(l + \frac{\langle\Delta\omega_\beta\rangle_\phi}{\omega_s}\right)\phi}, \\ \Omega^{(l)} &= \omega_{\beta,0} + l\,\omega_s + \langle\Delta\omega_\beta\rangle_\phi, \end{aligned} \qquad (5)$$

where $l \in \mathbb{Z}$ is the azimuthal mode number, and $\langle\Delta\omega_\beta\rangle_\phi(r)$ denotes the betatron frequency change $\Delta\omega_\beta(\delta(r,\phi))$ averaged over the longitudinal phase ϕ in the interval $[0, 2\pi)$. This quantity is, in general, dependent on the longitudinal amplitude r of the particles and thus describes the betatron frequency spread introduced through detuning with longitudinal amplitude. This term will eventually lead to Landau damping as demonstrated below when computing the dispersion relation. One can already see at this stage that $\langle\Delta\omega_\beta\rangle_\phi(r) \equiv 0$ for odd orders of chromaticity $\xi^{(2n+1)}$, $n \in \mathbb{N}_0$, i.e. the average frequency spread vanishes. This result is independent of the longitudinal particle distribution. Odd orders of chromaticity do not introduce Landau damping. On the other hand, even orders of chromaticity $\xi^{(2n)}$, $n \in \mathbb{N}$ introduce a betatron frequency spread with longitudinal amplitude that does not average out over time. In any case, though, both odd and even orders of chromaticity introduce a change of the effective impedance and modify the coherent frequencies of the modes which will also be demonstrated and discussed in the following section.

Having rewritten the Vlasov equation in terms of the azimuthal eigenmodes $G_1^l(r,\phi)$, one can multiply the result by $e^{-il\phi}$ and perform the integration over ϕ from 0 to 2π. Finally, one can integrate over r from 0 to ∞ to obtain Vlasov's equation in its 'final' form

$$\begin{aligned} \sigma_{lp} = -i\frac{q^2\omega_s\,\omega_0^2}{4\pi\omega_{\beta,0}E\eta} \sum_{l',\,p'=-\infty}^{\infty} \sigma_{l'p'}\, Z_1^\perp(\omega') \\ \times \int_0^\infty \frac{r g_0(r)\, \overline{H_l^{p'}}(r)\, H_l^p(r)}{\Omega^{(l)} - \omega_{\beta,0} - l\,\omega_s - \langle\Delta\omega_\beta\rangle_\phi(r)}\, dr, \end{aligned} \qquad (6)$$

where q is the electric charge of the particles, ω_0 the angular revolution frequency, and η the slip factor. Furthermore,

$$\begin{aligned} \sigma_{lp} &\doteq \int_0^\infty r R_l(r)\, H_l^p(r)\, dr, \\ H_l^p(r) &\doteq \frac{1}{2\pi}\int_0^{2\pi} e^{il\phi}\, e^{-\frac{i\omega'}{c} r\cos\phi}\, e^{-\frac{i}{\omega_s}B(r,\phi)}\, d\phi, \\ B(r,\phi) &\doteq \int_0^\phi \left[\Delta\omega_\beta(\delta(r,u)) - \langle\Delta\omega_\beta\rangle_\phi(r)\right] du, \end{aligned} \qquad (7)$$

with $l, p \in \mathbb{Z}$, and $\omega' \approx p'\omega_0 + \omega_{\beta,0} + l\,\omega_s$. In the weak-wake approximation, the summation over l' can be neglected and one can instead consider Eq. (6) as a set of independent equations in l. $H_l^p(r)$ can be perceived as a generalized Bessel function. It can be shown that in the event of a purely linear chromaticity, $H_l^p(r)$ reduces to the Bessel function of the first kind and Eq. (6) becomes identical to Eq. (6.179) in Ref. [18]. The phase terms $e^{-iB(r,\phi)/\omega_s}$ describe the alteration of the interaction of the beam with the impedance caused by arbitrary orders of chromaticity. The result is that the overlap sum over index p' in Eq. (6) between the $H_l^{p'}(r)$ functions and the impedance $Z_1^\perp(\omega')$ changes. This causes a change of the coherent frequencies $\Omega^{(l)}$, both for the real and imaginary components, of all the modes, an effect that is not related to Landau damping. Instead, Landau damping can be seen from the dispersion integral in the bottom line of Eq. (6). The incoherent detuning term $\langle\Delta\omega_\beta\rangle_\phi(r)$ in the denominator leads to an increase of the stable area in the complex frequency space as demonstrated in the following section. Equation (6) hence decouples the two beam dynamics effects introduced by nonlinear chromaticity and observed consistently in LHC experiments and in *PyHEADTAIL* simulations.

SOLUTIONS AND BENCHMARKS

This section discusses specific solutions to the previously derived Vlasov equation and summarizes the benchmarks performed to validate the formalism by means of the circulant matrix solver *BimBim* and the *PyHEADTAIL* tracking

ISBN: 978-3-95450-202-8 doi:10.18429/JACoW-HB2018-MOP2WA03

code. While the theory and the circulant matrix solver directly output the coherent frequencies for each azimuthal mode, the tracking results have to undergo additional post-processing. The real and imaginary parts of the coherent frequencies are obtained respectively from a SUSSIX frequency analysis and from exponential fits to the bunch centroid signals [19].

Equation (6) is first evaluated for a longitudinal airbag model where all the particles have the same longitudinal amplitude and hence there is no net frequency spread from any order of chromaticity. In that case, there is no Landau damping (the dispersion integral disappears from Eq. (6)) and one can thus study separately the change of the effective impedance. Thereafter, a longitudinal Gaussian bunch is analyzed where the two beam dynamics effects introduced by nonlinear chromaticity are both present. Here, even orders of chromaticity introduce a frequency spread and Landau damping. Stability boundary diagrams are computed and detailed comparisons with *PyHEADTAIL* tracking simulations are made.

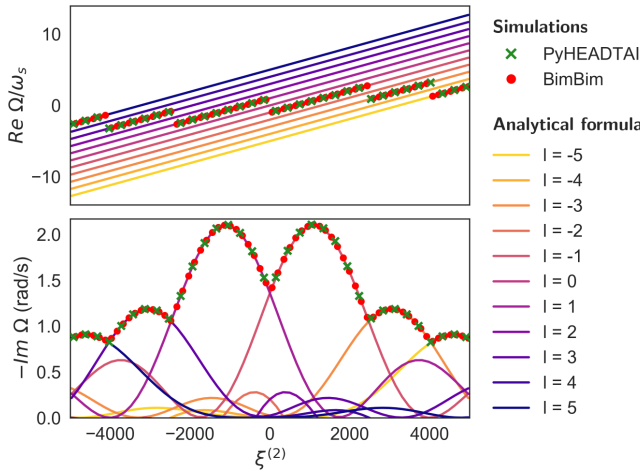

Figure 3: Real (top) and imaginary (bottom) coherent frequencies as a function of $\xi^{(2)}$ at fixed $\xi^{(1)} = 0.25$ for an airbag model using *BimBim* (red dots), *PyHEADTAIL* (green crosses), and analytical calculations (solid lines).

Airbag Model

To benchmark the developed theory against numerical models, a scan in second-order chromaticity is performed at fixed first-order chromaticity $\xi^{(1)} = 0.25$ for a longitudinal airbag distribution. The machine parameters used for the test are loosely based on the CERN Super Proton Synchrotron (SPS) at injection energy ($\gamma = 27.7$, $\omega_s/\omega_0 = Q_s = 0.017$, $\beta_z = 115\,\mathrm{m}$), where γ, Q_s, and β_z are the relativistic Lorentz factor, the (linear) synchrotron tune, and the longitudinal Courant-Snyder beta function respectively. The bunch intensity is at 10^9 p and the particles are set to have a longitudinal action of $J_z = 3\times10^{-4}$ m. A simple broad-band resonator impedance is used ($R_s = 10^7\,\Omega/\mathrm{m}$, $f_r = 0.8\,\mathrm{GHz}$, $Q = 1$), with R_s, f_r, Q respectively the resonator shunt impedance, its frequency, and its Q-value. Equation (6) is evaluated numerically and the results are plotted in Fig. 3 (solid lines) for azimuthal modes up to order $|l| = 5$. The theoretical predictions are in excellent agreement with the tracking (green crosses) and circulant matrix (red dots) models confirming the validity of the developed formalism. Also, the results demonstrate that second-order chromaticity modifies the effective impedance which leads to a change of the most unstable mode as a function of $\xi^{(2)}$. This effect was experimentally observed in the LHC. The real coherent frequency shifts are dominated by the constant (i.e. independent of r) and real-valued term $\langle\Delta\omega_\beta\rangle_\phi$ which is identical for all the azimuthal modes of an airbag beam.

Gaussian Beam

To study the effect of Landau damping from nonlinear chromaticity, a Gaussian beam is used for the comparison between the theory and the *PyHEADTAIL* model. For Gaussian beams, there is a longitudinal amplitude spread among the particles. In combination with even orders of chromaticity, this translates into a betatron frequency spread and an increase of the stability boundary diagram in the complex frequency space. In general, however, the eigenvalue problem in Eq. (6) is difficult to solve. To write down an analytical solution where the dispersion relation and Landau damping become more apparent, constraints are imposed on the shape of the impedance. A highly narrow-band resonator impedance is considered, for instance, such that effectively $Z_1^\perp(\omega') = Z_{p_0} \neq 0$ for $p' = p_0$, and $Z_1^\perp(\omega') = 0$ everywhere else. For this type of impedance, Eq. (6) simplifies greatly. To compute the stability boundary diagram, one considers the coherent frequency shift $\Delta\Omega_{\mathrm{lin}}^{(l)}$ in absence of Landau damping (*linear lattice*), determined by ignoring the frequency spread in Eq. (6). This yields

$$\left(\Delta\Omega_{\mathrm{lin}}^{(l)}\right)^{-1} = \frac{1}{\mathcal{N}}\int_0^\infty \frac{r g_0(r)\left|H_l^{p_0}(r)\right|^2}{\Omega^{(l)} - \omega_\beta(r) - l\,\omega_s}\,dr,$$
$$\mathcal{N} = \int_0^\infty r g_0(r)\left|H_l^{p_0}(r)\right|^2\,dr, \tag{8}$$

where $\omega_\beta(r) = \omega_{\beta,0} + \langle\Delta\omega_\beta\rangle_\phi(r)$. The dispersion relation is evaluated by adding a small complex part $i\varepsilon$ to the denominator of the integral (Landau bypass rule). By making additional assumptions on the beam spectrum and impedance, one can also show that Eq. (8) is equivalent to the results found by Scott Berg and Ruggiero in Ref. [16].

To benchmark Eq. (8) against *PyHEADTAIL*, the assumption on the strongly-peaked impedance needs to be fulfilled. This can be achieved by choosing a high quality factor resonator and tuning its frequency to match the spectral maximum of the azimuthal mode zero while remaining small for all the other modes. At the end of the tuning procedure, the values for the resonator were $R_s = 5\times10^{12}\,\Omega/\mathrm{m}$, $f_r = 0.7993\,\mathrm{GHz}$, and $Q = 5\times10^4$. Due to the high quality factor, multi-turn wakefield effects had to be enabled in *PyHEADTAIL*. A bunch length of $\sigma_z = 0.21$ m was used for

ISBN: 978-3-95450-202-8 doi:10.18429/JACoW-HB2018-MOP2WA03

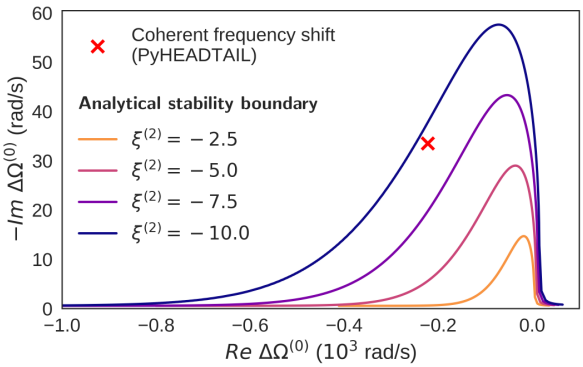

Figure 4: Stability boundary diagrams for different values of $\xi^{(2)}$ obtained by numerically solving the dispersion relation in Eq. (8). The coherent frequency shift of the mode under consideration is obtained from *PyHEADTAIL* (red cross).

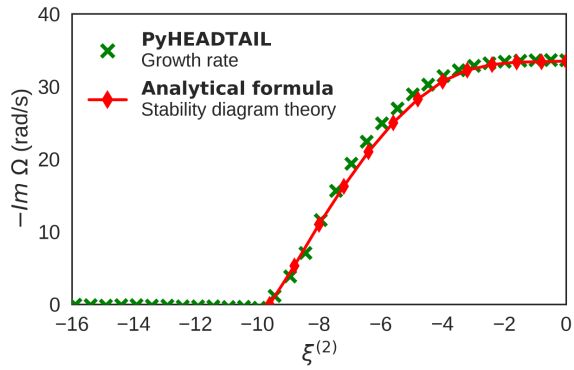

Figure 5: Stabilization of the head-tail mode zero as a function of $\xi^{(2)} < 0$ for a Gaussian beam. *PyHEADTAIL* simulations (green crosses) are shown together with predictions obtained from stability diagram theory (red diamonds).

the Gaussian distribution. All the other machine parameters were kept the same as above.

To evaluate beam stability analytically, the dispersion relation in Eq. (8) is solved numerically for different $\xi^{(2)}$. Solutions of the stability boundary diagrams are shown in Fig. 4 (solid lines) for four specific values of $\xi^{(2)}$. Due to the negative real part of the coherent frequency shift of the mode under consideration (red cross), negative values of $\xi^{(2)}$ are used as they provide stability more efficiently given the asymmetry of the frequency spread and of the stability diagrams. The plots illustrate the growth of the area of stability with increasing $|\xi^{(2)}|$. For $\xi^{(2)} \leq -10$, the area is large enough as to include the unstable mode from which point onwards it is fully Landau damped. It has been verified that by removing the frequency spread from the formula, the modes *cannot* be stabilized at least up to $|\xi^{(2)}| = 1000$. Furthermore, theoretical calculations show that within a few tens of units of $|\xi^{(2)}|$, there is no strong dependence of the coherent frequency on $\xi^{(2)}$, i.e. the change of effective impedance is insignificant here.

Figure 5 displays the dependence of the imaginary coherent frequency shift (instability growth rate) on the second-order chromaticity as obtained analytically (red diamonds) and from *PyHEADTAIL* simulations (green crosses). The analytical solutions were calculated using stability diagram theory: different values for $i\varepsilon$ were plugged in the denominator of Eq. (8) to compute the 'distortion' of the complex frequency space and therefore deduce the growth rates of the instability as a function of $\xi^{(2)}$. The *PyHEADTAIL* results were determined using exponential fits to the bunch centroid signals. The theory and the tracking model demonstrate an excellent agreement, not only on the stability threshold, but also on the evolution of the growth rate for intermediate $\xi^{(2)}$. It has also been verified that there is no other mode that becomes unstable, at least up to $|\xi^{(2)}| = 1000$.

CONCLUSIONS

The existing Vlasov theory on transverse dipole modes has been extended to include the effects of nonlinear chromaticity up to arbitrary order. This new formalism made it possible to confirm the hypothesis that nonlinear chromaticity has two effects on the beam dynamics of transverse coherent modes, observed in experiments with second-order chromaticity in the LHC: (i) it introduces Landau damping thanks to the incoherent betatron frequency spread with longitudinal amplitude, e.g. providing stability for single bunches in the LHC, and (ii) it alters the effective impedance, observed as a change of the most unstable mode in the LHC.

The theory has been successfully benchmarked up to second-order chromaticity for an airbag model and a Gaussian beam using a tracking model and a circulant matrix solver. All the benchmarks revealed an excellent agreement with the theory. For the Gaussian beam it has been shown that, given the assumption of a strongly-peaked impedance, analytical predictions from stability diagram theory are in perfect agreement with tracking simulations. This proves that detuning with longitudinal amplitude indeed provides Landau damping. The frequency spread can be introduced for example with even orders of chromaticity, or, similarly, with an rf quadrupole. This is in accordance with experiments and simulations that were carried out on the rf quadrupole and on second-order chromaticity in the LHC, confirming the interpretation of these results.

ACKNOWLEDGMENTS

The authors thank R. De Maria and G. Rumolo for important contributions to these studies and the LHC OP teams for their support during the experiments.

REFERENCES

[1] L. Landau, "On the vibration of the electronic plasma", *J. Phys. USSR*, vol. 10, pp. 25–34, 1946.

[2] M. Benedikt and F. Zimmermann, "Future Circular Colliders", CERN, Geneva, Switzerland, Rep. CERN-ACC-2015-0164, Jul. 2015.

[3] A. Grudiev, "Radio frequency quadrupole for Landau damping in accelerators", *Phys. Rev. ST Accel. Beams*, vol. 17, p. 011001, Jan. 2014.

ISBN: 978-3-95450-202-8 doi:10.18429/JACoW-HB2018-MOP2WA03

[4] M. Schenk, A. Grudiev, K. Li, K. Papke, "Analysis of transverse beam stabilization with radio frequency quadrupoles", *Phys. Rev. Accel. Beams*, vol. 20, p. 104402, Oct. 2017.

[5] E. Métral *et al.*, "Beam instabilities in hadron synchrotrons", *IEEE Transactions on Nuclear Science*, vol. 63, no. 2, pp. 1001–1050, Apr. 2016.

[6] M. Schenk *et al.*, "Practical stabilisation of transverse collective instabilities with second order chromaticity in the LHC", *in Proc. 8th Int. Particle Accelerator Conf. (IPAC'17)*, Copenhagen, Denmark, May 2017, paper THPVA026, pp. 4477–4480.

[7] O. Brüning *et al.*, "LHC Design Report", CERN Yellow Reports: Monographs, CERN, Geneva, Switzerland, CERN-2004-003-V-1, Jun. 2004.

[8] L. R. Carver *et al.*, "MD1831: Single bunch instabilities with Q'' and non-linear corrections", CERN, Geneva, Switzerland, CERN-ACC-NOTE-2017-0012, Feb. 2017.

[9] V. V. Danilov and E. A. Perevedentsev, "Feedback system for elimination of the transverse mode coupling instability", *NIM A*, vol. 391, no. 1, pp. 77–92, 1997.

[10] X. Buffat, "Transverse beams stability studies at the Large Hadron Collider", Ph.D. thesis, LPAP, École Polytechnique Fédérale de Lausanne (EPFL), Lausanne, Switzerland, 2015.

[11] L. R. Carver *et al.*, "Current Status of Instability Threshold Measurements in the LHC at 6.5 TeV", *in Proc. 7th Int. Particle Accelerator Conf. (IPAC'16)*, Busan, Korea, May 2016, paper TUPMW011, pp. 1434–1437.

[12] L. R. Carver *et al.*, "MD1228: Validation of Single Bunch Stability Threshold & MD1751: Instability Studies with a Single Beam", CERN, Geneva, Switzerland, Rep. CERN-ACC-NOTE-2017-0013, Feb. 2017.

[13] J. Gareyte, J.-P. Koutchouk, F. Ruggiero, "Landau damping, dynamic aperture and octupoles in LHC", CERN, Geneva, Switzerland, Rep. CERN-LHC-Project-Report-91, Feb. 1997.

[14] N. Mounet, "The LHC Transverse Coupled-Bunch Instability", Ph.D. thesis, LPAP, École Polytechnique Fédérale de Lausanne (EPFL), Lausanne, Switzerland, 2012.

[15] Methodical Accelerator Design, mad.web.cern.ch.

[16] J. S. Berg and F. Ruggiero, "Stability diagrams for Landau damping", *in Proc. 17th Particle Accelerator Conf. (PAC'97)*, vol. 2, Vancouver, B.C., Canada, May 1997, pp. 1712–1714.

[17] T. Levens *et al.*, "Instability diagnostics", *in Proc. 2015 Evian Workshop on LHC beam operation*, Evian, France, Dec. 2015, CERN-ACC-2015-376, pp. 137–141.

[18] A. W. Chao, *Physics of collective beam instabilities in high energy accelerators*, Wiley Series in Beam Physics and Accelerator Technology, Wiley, 1993.

[19] R. Bartolini and F. Schmidt, "A Computer Code for Frequency Analysis of Non-Linear Betatron Motion", CERN, Geneva, Switzerland, Rep. SL-Note-98-017-AP, Feb. 1998.